Indian Journal of Engineering & Materials Sciences
Vol. 31, October 2024, pp. 742-749
DOI: 10.56042/ijems.v31i5.9435

On the structural study, I-V measurements and observation of Meyer-Neldel rule in Sb additive Se-Te glassy alloys

Balbir Singh Patial*[a], Nitin Kumar[a], Anita Kumari[b] & Nagesh Thakur[a]

[a]Department of Physics, Himachal Pradesh University Summerhill, Shimla, H.P.171 005, India

[b]Department of Chemistry, GGDSD College Rajpur (Palampur), District Kangra, H.P. 176 067, India

Received: 9 March 2024; accepted: 12 July 2024

In the present paper, the samples under investigation $Se_{80-x}Te_{20}Sb_x$ (x = 2, 4 and 8) have been prepared by melt-quench procedure. The structural study has been made using x-ray diffraction (XRD), scanning electron microscopy (SEM) and energy dispersive analysis of X-ray (EDAX). Semiconducting nature of these glasses has been studied by current-voltage (I-V) measurements. *dc* conductivity measurements, linear and non-linear behaviour and observation of Meyer-Neldel rule have been done at temperature range between 303 K and 333 K in the voltage range upto 200V. From I-V curves, linear and non-linear behaviour has been investigated. It is evident from the analysis that conductivity is increasing with increasing temperature. It is also established that Meyer- Neldel rule is obeyed by these glasses.

Keywords: Structural, Current Voltage, Meyer-Neldel rule

1 Introduction

In the field of materials science, the semiconductor field always remained the field of versatility and significance. The recent trend of advancing technology imposed the rigorous requirement of innovation in semiconductor science. Therefore, the emphasis also shifts upon the amorphous semiconductors, especially on the chalcogenide glasses as these offer a wide-range tailoring of the thermal, electrical and optical properties. According to technological applications, these glasses have wide range of applications in memory switching devices, thermal imaging, solar cells, photonic crystals and other photonic applications. In order to explore the technological applications of the materials, we need to study its electrical, thermal and optical behaviour. Amongst amorphous chalcogenide glasses, Se-based systems are very useful in optical memory switching rectifiers and photocells due to the observation of reversible transformation[1] and hence seem attractive. However, in pure state, Se-based alloys were found to be thermally unstable and to have limited reversibility[2]. In order to improve the properties of Se glassy system, various efforts have been made by the different researchers and the elements such as Te, Sb, Sn, Pb, Bi have been added. Antimony is a good suitable tailoring agent to tune the physical properties of a material for a particular technological application. The weaker bond strength of Se-Sb bonds and steric hindrance introduced by large size of Sb causes strain and weakens the glass matrix, which opens the possibility to reduce the gap between the melting and peak crystallization temperature and makes it suitable for phase change materials.

The chalcogenide glasses are gradually becoming promising materials in scientific research owing to there are some unusual properties including excellent chemical stability in aggressive environments, low phonon energy, high photosensitivity, high thermal stability, high refractive index, extended infrared transparency, exclusive chemical durability and unique nonlinear optical properties along with potential applications such as x-ray imaging and photonic applications[2,3]. The direct current (*dc*) conductivity measurements of amorphous semiconductors have attracted great deal of attention to understand the conduction process in these materials. Thus, the study of electrical behaviour of these materials is extremely important.

The Meyer-Neldel Rule (MNR), which is also known as "compensation effect" was established empirically in 1937[4]. The MNR is often observed in an activated process. In semiconductors, electrical

*Corresponding author
(E-mail: bspatial@gmail.com, bspatial@hpuniv.ac.in)

conductivity is temperature dependent, although the creation of defect levels influences the spread of activation energy[5]. However, at a characteristic MNR temperature, this process becomes independent of dopant concentration or activation energy[6,7]. To analyse the origin of the MNR, various mechanisms have been proposed. Many researchers attributed that the MNR is a consequence of disorder effect, transport mechanism, multi-trapping transport process etc. within the materials[6,8-9]. The most interesting feature of Meyer-Neldel Rule is that it has been observed in various materials, including amorphous, crystalline, liquid semiconductors, polycrystalline, solid state ion conductors and organic solids, as well as for variety of properties including thermal crystallization, conductivity, surface desorption, diffusion and adsorption kinetics. Moreover, MNR is frequently investigated in disordered materials[10]. In most chalcogenide systems, MNR is studied by activation energy (ΔE) variation with composition of glassy system. For this purpose, electrical conductivity is evaluated as the function of temperature. In specific glassy alloys, when composition varies, (ΔE) changed; hence the density of defect states and their distribution with energy varies with compositional disorder[11]. The density of defect states and their distribution determine the statistical shift, which may be responsible for MNR in chalcogenide systems. Many researchers have been reported that ΔE changes with varying voltage in the high field region, where the density of defect states remains unchanged with varying ΔE[11]. As a consequence, the MNR is important for the design and applications of chalcogenide glasses as observed by various researchers[6,11].

According to Pichon et al.[12], it could be a diagnostic tool to quantify the quality of active layer. In phthalocyanine thin films, Abdul-Wahab[13] proposed the use of Meyer-Neldel behaviour for oxidizing gas detection. Widenhorn et al.[14] suggested that in silicon diode, the MNR could be implemented to describe the temperature dependence of forward current. In amorphous $InGaZnO_4$ thin-film transistors (a-IGZO TFTs), Takechi et al[15] reported that MNR combined with an exponential tail-state distribution model can be implemented to explain the sub threshold characteristics. In phase change memory (PCM) devices, Ielmini et al.[16] suggested that MNR can be used to analyse the crystallization and structural relation. Similarly, the interpretation and consequence of MNR for conductivity of a large number of memory cells of a GeSbTe phase-change memory alloy is reported by Savransky and Yelon[17]. Moreover, Okamoto et al.[18] derived generalized MN relations in term of Laplace transform.

In the present work, semiconducting nature of $Se_{80-x}Te_{20}Sb_x$ (x = 2,4 and 8) glassy alloysis studied by current-voltage (I-V) measurements. *dc* conductivity measurements, linear and non-linear behaviour and observation of Meyer-Neldel rule are investigated at temperature range between 303 K and 333 K in the voltage range 0–200V. The structure and surface morphology are studied by X-ray diffraction (XRD), scanning electron microscopy and energy dispersive analysis of X-rays (EDAX) of the investigated glassy alloys.

The Meyer-Neldel Rule (MN-rule)

In case of a chalcogenide system, the MN-rule states that the thermally activated *dc* electrical conduction (σ) obeys the Arrhenius relation:

$$\sigma = \sigma_o \exp\left(-\frac{\Delta E}{k_B T}\right) \quad \text{...(1)}$$

where ΔE and σ_o are activation energy and pre-exponential factor respectively and k_B is the Boltzmann constant. It has been observed that σ_o does not depend on ΔE for many materials. Taking log on both sides in equation (1)

$$ln\sigma = ln\left(\sigma_o \exp\left(-\frac{\Delta E}{k_B T}\right)\right) \quad \text{...(2)}$$

$$ln\sigma = ln\sigma_o + ln\left(exp\left(-\frac{\Delta E}{k_B T}\right)\right) \quad \text{...(3)}$$

$$ln\sigma = ln\sigma_o - \frac{\Delta E}{k_B T} \quad \text{...(4)}$$

$$ln\sigma = ln\sigma_o - \left(\frac{\Delta E}{k_B}\right)\left(\frac{1}{T}\right) \quad \text{...(5)}$$

This is the equation of straight line like $y = mx + c$, where $m = -\Delta E/k_B$; and $ln\sigma_o$ is the intercept.

If logarithm of the conductivity is plotted on the ordinate against the reciprocal of the absolute temperature, then a straight line is generated whose slope is $\Delta E/k_B$ and the extrapolated intercept of the line on the ordinate at $T^{-1} = 0$ yields the value of $ln\sigma_o$.

We have a contradiction that if equation (1) is correct, then it would require that $\sigma(T) = \sigma_o$ if either $T \to \infty$ *or* a multiplicity of σ_o values are found. Thus,

$$\sigma_o = \sigma_{oo} exp\left(\frac{\Delta E}{k_B T_{MN}}\right) \quad \text{...(6)}$$

$$\sigma_O = \sigma_{OO} exp\left(\frac{\Delta E}{E_{MN}}\right) \quad \ldots(7)$$

where σ_{oo} and $E_{MN} = k_B T_{MN}$ (T_{MN} denotes specific temperature) are constants. E_{MN} and σ_{oo} are called as Meyer-Neldel energy and Meyer-Neldel pre-exponential factor respectively. Here equation (7) is referred to as a Meyer Neldel relation (MNR).

Shimakawa and Abdel-wahab observed a more surprising and interesting result while studying the MNR in different chalcogenide glassy systems. In case of chalcogenide glasses, they reported a strong correlation between σ_{oo} and E_{MN}, which can be expressed as:

$$ln\sigma_{oo} = \alpha + \beta E_{MN} \quad \ldots(8)$$

where α and β are constants. This expression between σ_{oo} and E_{MN} is known as "Further MNR".

2 Materials & Methods

Amorphous $Se_{80-x}Te_{20}Sb_x$ (x = 2, 4 and 8) glassy alloys were obtained using melt-quench procedure mentioned elsewhere 19. Structural study is carried out using XRD, SEM and EDAX.

Pellets of the powdered samples with diameter ≈10mm and thickness ≈1mm were obtained using a die by applying a pressure of 5 ton. Each pellet was coated with silver paste to achieve good electrical contact between sample and electrode. *dc* conductivity measurements of primed samples were carried out in the temperature range 293 K to 313 K. A *dc* voltage of 0-200 V was applied across the sample for *I–V* measurements and the resultant current was monitored with a digital picometer (Keithley 2611 model). Before completing any *I–V* measurement, each temperature was given at least 10 minutes of stabilisation time.

2.1 Structural Study

The structure and surface morphology of $Se_{80-x}Te_{20}Sb_x$ (x = 2, 4 and 8) were examined by XRD technique and scanning electron microscope (SEM) and elemental composition is verified by EDAX.

2.1.1 X-ray diffraction (XRD)

For XRD analysis of glassy alloy in the bulk form, the investigated sample were crushed into fine powder form with a pestle and mortar. The powder technique was used to obtain XRD patterns of the materials under study. Figures 1-3 show the X-ray diffraction pattern of the investigated chalcogenide $Se_{80-x}Te_{20}Sb_x$ (x = 2, 4 and 8) glasses. The absence of any sharp peak or prominent peak in XRD pattern confirmed the amorphous nature of chalcogenide glasses under analysis.

2.1.2 Scanning Electron Microscope (SEM) Measurements

The scanning electron microscope is used to study the surface morphology and the structure of the

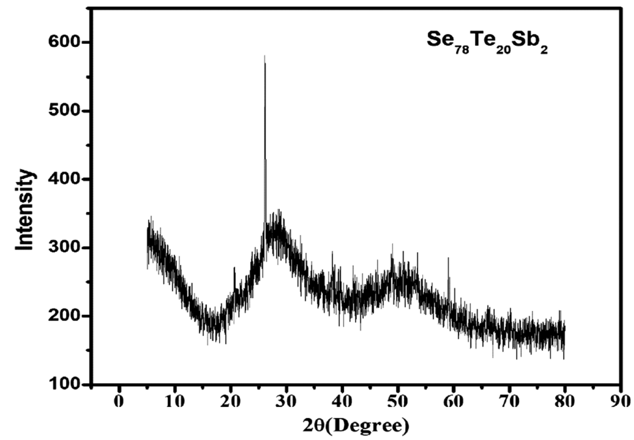

Fig. 1 — XRD pattern of chalcogenide $Se_{78}Te_{20}Sb_2$ glass.

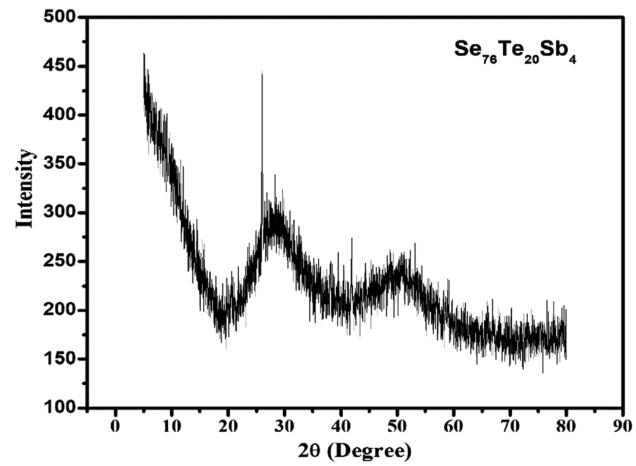

Fig. 2 — XRD pattern of chalocogenide $Se_{76}Te_{20}Sb_4$ glass.

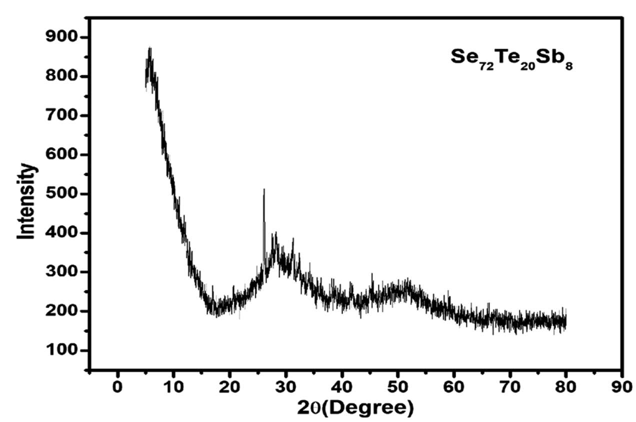

Fig. 3 — XRD pattern of chalcogenide $Se_{72}Te_{20}Sb_8$ glass.

materials. Figures 4 - 6 show the SEM images of $Se_{80-x}Te_{20}Sb_x$ (x= 2, 4 and 8) samples of the series under study. The irregular edges (Figures 4-6) are consistent with amorphous nature of these particles. Scanning electron microscopy is the technique which is used to study the inhomogeneity in the sample. There is an indication of the partial phase separation in the materials due to inhomogeneity in the samples as observed from the SEM micrographs shown in Figs (4 – 6).

2.1.3 Energy Dispersive Analysis of X-ray (EDAX)

EDAX is also known as energy dispersive spectroscopy and can also be abbreviated as EDS, EDX, EDXS or XEDS sometimes it is termed energy dispersive X-ray microanalysis (EDXMA) or energy dispersive X-ray analysis (EDXA). It's an investigative method which is widely employed in elemental or chemical composition characterization of materials. The sample may be of any form such as solid thin film, solid powder, liquid sample, even a pellet etc. Figures 7-9 present the EDAX graphs followed by chemical composition data for all the investigated samples. For the compositional analysis, the constitutional elements Se, Te and Sb has been taken as reference samples. The composition of the bulk samples is found to be uniform within the measurement accuracy of about ±2%.

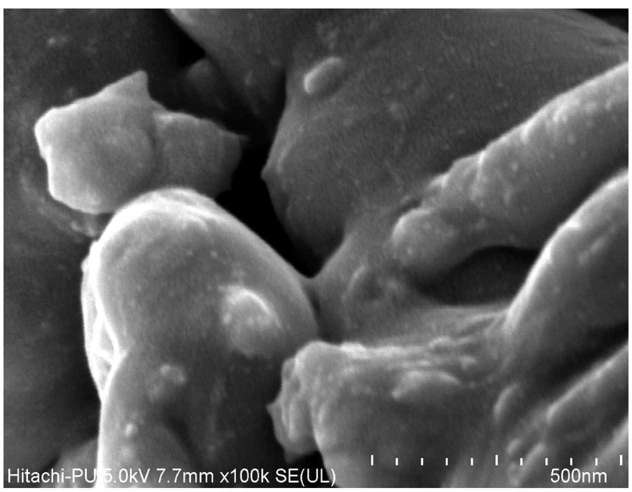

Fig. 4 — SEM image of chalcogenide $Se_{78}Te_{20}Sb_2$ glass.

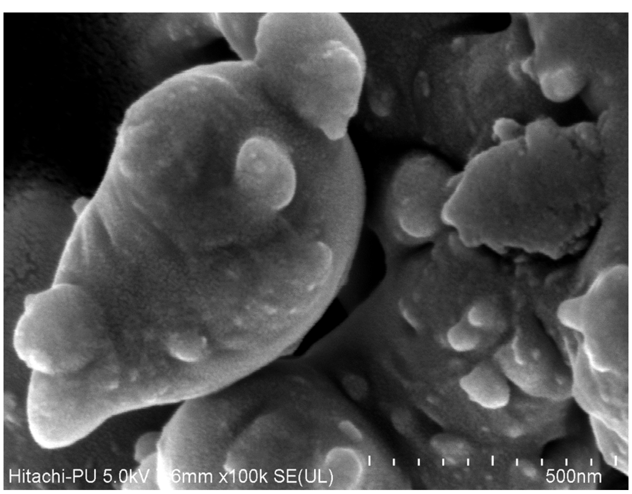

Fig. 5 — SEM image of chalcogenide $Se_{76}Te_{20}Sb_4$ glass.

2.2 Electrical Measurements

Current-voltage (I-V) characteristics and *dc* electrical conductivity measurements are made for

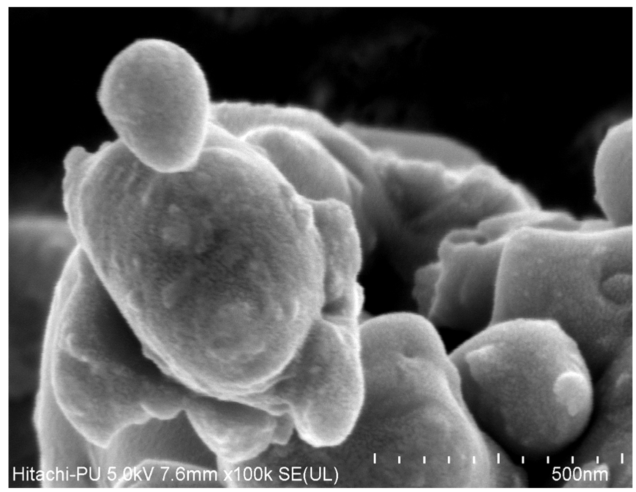

Fig. 6 — SEM image of chalcogenide $Se_{72}Te_{20}Sb_8$ glass.

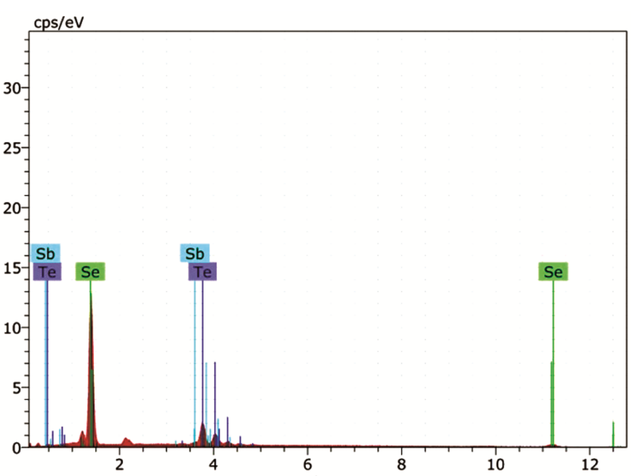

Ident-Spectrum Date:4/21/2022 8:15:22 PM HV:15.0kV Puls th.:4.18kcps

Spectrum: test 12281

Element	Series	unn. C [wt.%]	norm. C [wt.%]	Atom. C [at.%]	Error (3 Sigma) [wt.%]
Selenium	L-series	46.39	65.81	75.61	6.95
Tellurium	L-series	22.31	31.66	22.50	2.10
Antimony	L-series	1.79	2.53	1.89	0.29
	Total:	70.48	100.00	100.00	

Fig. 7 — EDAX analysis of $Se_{78}Te_{20}Sb_2$.

$Se_{80-x}Te_{20}Sb_x$ (x = 2,4 and 8) pellets. The typical I-V characteristics are recorded from room temperature to elevated temperatures up to 333 K. I-V characteristics show ohmic behaviour in the low voltage range and this behaviour turns to non-ohmic in the higher voltage range due to high voltage induced temperature effects. Meyer-Neldel (MN) rule is also explained for our present system of chalcogenide glasses.

2.2.1 I-V Measurements

Figures 10-12 show I-V characteristics for investigated composition at different temperatures. It is clear from figure 10 that current is increasing with applied voltage when temperature is fixed and with temperature when applied voltage is fixed. The behaviour of these samples shows semiconducting nature and I-V curves show linear behaviour in the voltage range 0-50 V while at high voltage range, they deviate from linearity i.e. non-ohmic behaviour is observed.

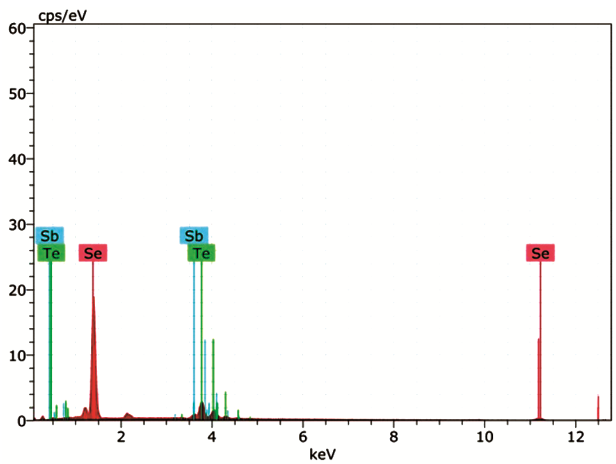

Ident-Spectrum Date:4/21/2022 8:06:27 PM HV:15.0kV Puls th.:6.39kcps

Spectrum: test 12277

Element	Series	unn. C [wt.%]	norm. C [wt.%]	Atom. C [at.%]	Error (3 Sigma) [wt.%]
Selenium	L-series	46.91	64.96	74.82	7.00
Tellurium	L-series	20.92	28.97	20.65	1.94
Antimony	L-series	4.38	6.06	4.53	0.49
	Total:	72.21	100.00	100.00	

Fig. 8 — EDAX analysis of $Se_{76}Te_{20}Sb_4$.

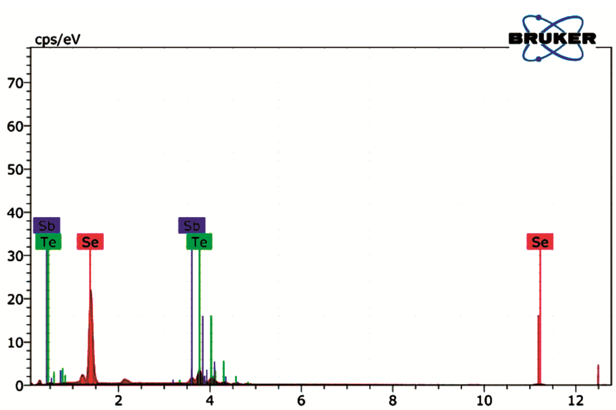

Spectrum: test 12276

Element	Series	unn. C [wt.%]	norm. C [wt.%]	Atom. C [at.%]	Error (3 Sigma) [wt.%]
Selenium	L-series	45.73	62.20	72.38	6.83
Tellurium	L-series	19.43	26.43	19.03	1.82
Antimony	L-series	8.36	11.38	8.59	0.86
	Total:	73.53	100.00	100.00	

Fig. 9 — EDAX analysis of $Se_{72}Te_{20}Sb_8$.

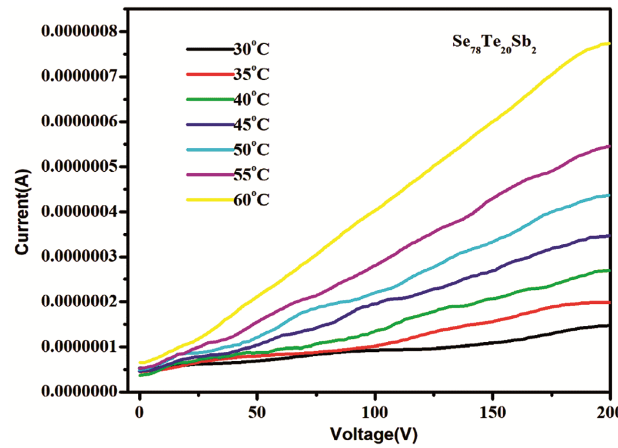

Fig. 10 — I-V measurements of chalcogenide $Se_{78}Te_{20}Sb_2$ glass.

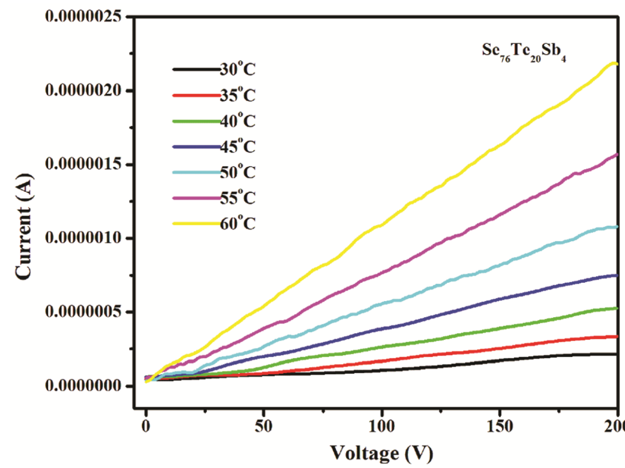

Fig. 11 — I-V measurements of chalcogenide $Se_{76}Te_{20}Sb_4$ glass.

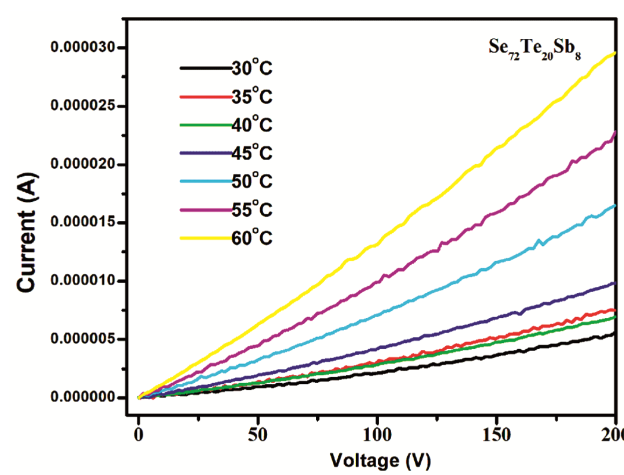

Fig. 12 — I-V measurements of chalcogenide $Se_{72}Te_{20}Sb_8$ glass.

Table 1 — Value of resistance (R) and *dc* conductivity (σ_{dc}) for $Se_{80-x}Te_{20}Sb_x$ (x = 2, 4 and 8) glasses in ohmic region at different temperatures.

	$Se_{78}Te_{20}Sb_2$		$Se_{76}Te_{20}Sb_4$		$Se_{72}Te_{20}Sb_8$	
Temperature (°C)	Resistance (Ω)	σ_{dc} ($\Omega^{-1}cm^{-1}$)	Resistance (Ω)	σ_{dc} ($\Omega^{-1}cm^{-1}$)	Resistance (Ω)	σ_{dc} ($\Omega^{-1}cm^{-1}$)
30	2.45×10^{-10}	4.15×10^{-11}	2.73×10^{-10}	3.40×10^{-11}	1.83×10^{-8}	2.07×10^{-8}
35	2.74×10^{-10}	4.64×10^{-11}	5.98×10^{-10}	7.44×10^{-11}	2.55×10^{-8}	2.89×10^{-8}
40	3.98×10^{-10}	6.76×10^{-11}	1.22×10^{-10}	1.52×10^{-11}	2.54×10^{-8}	2.87×10^{-8}
45	7.26×10^{-10}	1.23×10^{-10}	1.74×10^{-9}	2.16×10^{-10}	3.93×10^{-8}	4.44×10^{-8}
50	1.99×10^{-10}	3.38×10^{-10}	2.70×10^{-9}	3.35×10^{-10}	6.45×10^{-8}	7.29×10^{-8}
55	2.45×10^{-10}	4.15×10^{-10}	3.68×10^{-9}	4.57×10^{-10}	9.04×10^{-8}	1.02×10^{-7}
60	1.83×10^{-9}	3.10×10^{-10}	5.41×10^{-9}	6.73×10^{-10}	1.25×10^{-7}	1.41×10^{-7}

The slope of I-V plots gives the apparent values for *dc* resistance (R). For $Se_{80-x}Te_{20}Sb_x$ (x = 2,4 and 8) investigated system, *dc* conductivity in ohmic region is evaluated by the relation given below.

$$\sigma_{dc} = \frac{1}{\rho_{dc}} = \left(\frac{1}{R}\right)\left(\frac{L}{A}\right) \quad \ldots(9)$$

Here L denotes thickness, A indicates area of cross-section, and ρ_{dc} represents the resistivity of the material.

The thickness of the pellets $Se_{80-x}Te_{20}Sb_x$ (x = 2,4 and 8) is 0.15 cm, 0.11cm, 0.10 cm respectively and the area of cross-section is 1.1304 cm^2 for each pellet.

2.2.2 Observation of Meyer -Neldel Rule

In case of glassy semiconductors, MN rule is observed by the variation of activation energy on the changing the composition of the glassy alloys in a specific glassy system. The temperature dependent *dc* conductivity (σ_{dc}) of $Se_{80-x}Te_{20}Sb_x$ (x = 2,4 and 8) in the temperature range of 303 to 333 K is measured (Table 1). It is found that *dc*conductivity increases exponentially over the entire temperature range. Figures 13-15 show the temperature dependence of *dc* conductivity for$Se_{80-x}Te_{20}Sb_x$ (x =2,4 and 8) glasses in the considered temperature range. *dc* conductivity varies exponentially with temperature according to equation (5) and it can be seen in $ln\sigma_{dc}$ versus 1000/T plots. Theseplots show thermally activated phenomenon.

Figures 13–15 show that the *dc* conductivity increases with the increase in temperature. From the slope and intercept, ΔE and σ_o is calculated. The values of activation energy and $ln\ \sigma_o$ in the studied temperature range are shown in Table 2. It shows the semiconducting nature of the amorphous materials. The composition dependence of activation energy is shown in Fig. 16. It is observed from Fig. 16 that the activation energy is increased from x = 2 to x = 4 but there is a sharp decrease for x = 8.

Table 2 — Activation energy and $ln\sigma_o$ for $Se_{80-x}Te_{20}Sb_x$ (x=2,4 and 8) glassy alloys.

Composition	ΔE (eV)	$ln\sigma_o$ ($\Omega^{-1}cm^{-1}$)
$Se_{80}Te_{18}Sb_2$	0.75	4.5464812
$Se_{80}Te_{16}Sb_4$	0.83	8.0864103
$Se_{80}Te_{12}Sb_8$	0.56	4.0271358

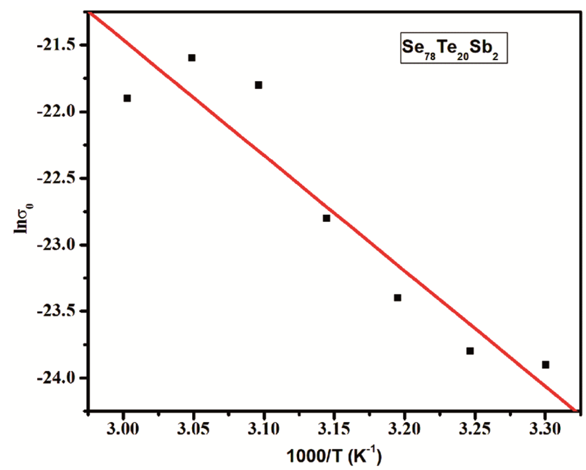

Fig. 13 — Temperature dependence of dc conductivity in $Se_{78}Te_{20}Sb_2$.

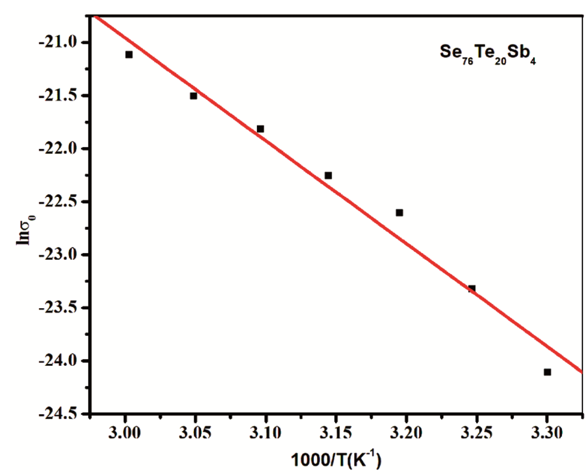

Fig. 14 — Temperature dependence of dc conductivity in $Se_{76}Te_{20}Sb_4$.

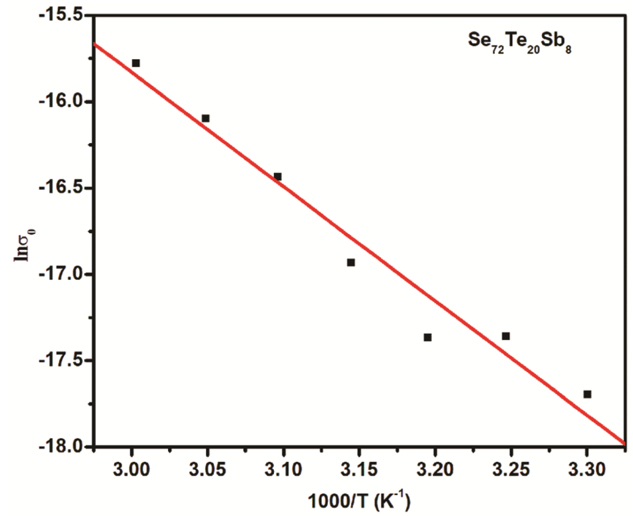

Fig. 15 — Temperature dependence of dc conductivity in $Se_{72}Te_{20}Sb_8$.

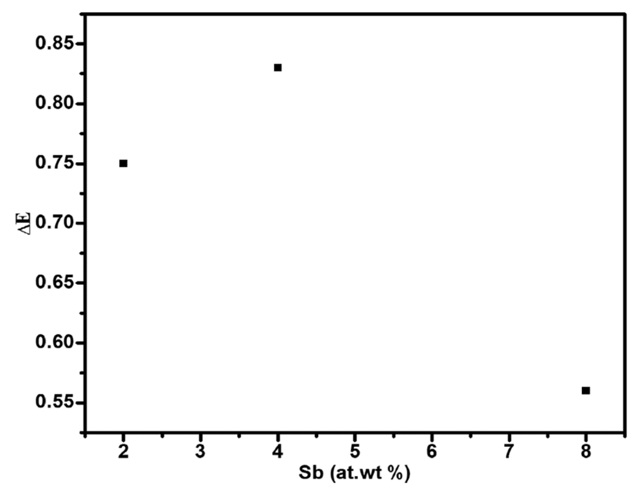

Fig. 16 — Composition dependence of activation energy of chalcogenide $Se_{80-x}Te_{20}Sb_x$ (x = 2,4 and 8) glasses.

It is observed that σ_o is not constant for the series under study. The value of σ_o increases as the activation energy increases for (x = 2, 4 and 8). In case of x = 8 atomic weight percentage, the value of σ_o decreases as the activation energy decreases. Figure 17 shows the plot between $ln\,\sigma_o$ and ΔE that $ln\sigma_o$ varies exponentially with ΔE according to relation given by equation (5) and MN rule is obeyed in the present system. The slope and intercept of the line yield Meyer-Neldel characteristics energy E_{MN} = 14.89 meV and MN pre- exponential factor is equal to 2.78 × 10^{-2} $\Omega^{-1}cm^{-1}$ which is close to the given range of Meyer- Neldel energy and pre- exponential factor.

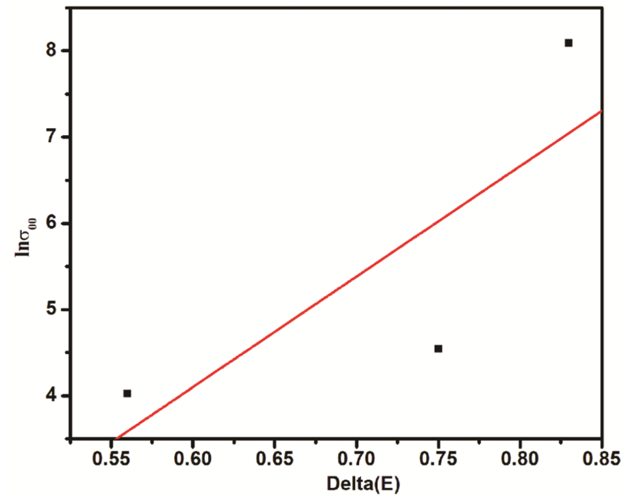

Fig. 17 — Plot of $ln\sigma_o$ versus ΔE of chalcogenide $Se_{80-x}Te_{20}Sb_x$ (x = 2, 4 and 8) glasses.

3 Conclusion

The glasses of the desired composition i.e. $Se_{80-x}Te_{20}Sb_x$ (x = 2,4 and 8) were prepared by using melt quenching technique. To confirm the amorphous nature of these samples, XRD characterization is carried out and the absence of any sharp peak in the XRD patterns of these samples confirm their amorphous nature. Surface morphology of glassy alloys is investigated by using scanning electron microscope (SEM). The irregular edges of the particle are consistent with amorphous nature of these particles and inhomogenity in the samples is observed in SEM micrographs.

For I-V measurements in bulk, pellets of $Se_{80-x}Te_{20}Sb_x$ (x = 2,4 and 8) glassy alloy are prepared. From I-V curves, linear and non-linear behaviour is investigated. We have studied *dc* conductivity, and Meyer-Neldel rule in the voltage range 0–200 V. It is clearly evident in these curves that conductivity is increasing with increasing the temperature which shows the semiconductor nature of the sample. Maximum value of dc conductivity is found for x = 8 sample in the investigated composition. The increase in the conductivity with the increase of Sb content indicates that the samples may be more useful in optoelectronic devices.

From $ln\sigma_{dc}$ versus 1000/T, we calculate the value of activation energy. It is found that the plot exhibits Arrhenius behaviour in the studied temperature range (303 – 333 k). It is thermally activated phenomenon. It is also established that Meyer- neldel rule is obeyed by these glasses. Meyer-Neldel characteristics energy

E_{MN} = 14.89 meV and MN pre- exponential factor is equal to 2.78 × 10^{-2} $\Omega^{-1}cm^{-1}$ which is close to the given range of Meyer- Neldel energy and pre-exponential factor suggested by Shimakawa and Abdul – Waheb for chalcogenide glasses.

References

1 Kumar S & Singh K, *Physica B*406 (8) (2011) 1519.
2 Thakur A, Patial B S & Thakur N, *J Electron Mater*, 46 (2007) 1516.
3 Esakkiraj E, Mohanraj K, Sivakumar G & Henry J, *Optik,* 126 (19) ((2015) 2133.
4 W. Meyer, and H. Neldel, *Z. Tech. Physics,* 12 (1937) 588.
5 Gupta V, Bhattacharya P, Yu. I. Yuzuk YI, Sreenivas K & Katiyar RS, *J Cryst Growth,*287 (1) (2006)39.
6 Sagar P, Kumar M &Mehra RM, *Solid State Commun*, 147 (11-12) (2008) 465.
7 Crandall RS, *Phys Rev,* B 43 (1991) 4057.
8 Chen YF & Huang SF, *Phys. Rev.* B 44 (1991) 13775.
9 Yelon A & Movaghar B, *Phys Rev Lett* 65(1990) 618.
10 Dwivedi S K, Dixit M & Kumar A, *J Mater Sci Lett* 17 (1998) 233.
11 Anjali, Patial BS, Chand S & Thakur N, *J Mater Sci Mater Electron,* 31 (2020) 2741.
12 Pichon L, Mercha A, Routoure JM, Carin R, Bonnaud O & Mohammed-Brahim T, *Thin Solid Films,* 427 (1-2) (2003) 350.
13 Fouad Abdel-Wahab, *J Appl Phys,* 91(2002) 265.
14 Widenhorn R,Fitzgiibbons M & Bodegom EJ, *J Appl Phys,* 96 (2004)7379.
15 Takechi K, Nakata M, Eguchi T, Yamaguchi H & Kaneko S, *Jpn J Appl Phys,* 48 (2009) 078001.
16 Ielmini D, Boniardi M, Lacaita AL, Redaelli A & Pirovano A, *Microelectron Eng,* 86 (2009) 1942.
17 Savransky SD &Yelon A, *Phys Status Solidi* A, 207 (2010) 627.
18 Okamoto H,Sobajima Y, Toyama T & Matsuda A, *Phys Status Solidi* A, 207 (2010) 566.
19 Patial B S, Thakur N & Tripathi S K, *Thermochim Acta,* 513 (2011) 1.